Influence of Premade and In Situ Compatibilizers in Polypropylene/Ethylene–Propylene–Diene Terpolymer Thermoplastic Elastomeric Olefins and Thermoplastic Vulcanizates

K. Naskar, J. W. M. Noordermeer

Department of Rubber Technology, Faculty of Chemical Technology, Dutch Polymer Institute, University of Twente, P.O. Box 217, 7500 AE Enschede, The Netherlands

ABSTRACT: During dynamic vulcanization of polypropylene (PP)/ethylene–propylene–diene terpolymer (EPDM) blends with dicumyl peroxide/triallyl cyanurate, there is a possibility of the generation of in situ graft links at the interface. Three potential compatibilizers (PP-grafted EPDM, styrene–ethylenebutylene–styrene, and *trans*-polyoctenamer) for PP/EPDM blends were first investigated as references to obtain a quantified insight into the effects to be expected from in situ graft links. Only the first compatibilizer showed some compatibilizing action in straight, unvulcanized blends, as evidenced by a slight increase in the tensile strength of the blend and a somewhat smaller EPDM particle size within the PP matrix. Also, dynamic mechanical testing, in particular, the glass-transition temperatures of the PP and EPDM components, showed some signs of compatibilization. The PP-grafted EPDM resembled most closely the structures of PP and EPDM. In the spectra obtained with high temperature, solid-state NMR, there was an indication that PP–EPDM graft links were generated during the dynamic vulcanization process that still remained after the extraction of the free PP phase from the thermoplastic vulcanizate film. NMR relaxation experiments gave further evidence for the graft links formed in situ. In all cases, only qualitative indications could be achieved because of the extremely low number of graft links formed. © 2006 Wiley Periodicals, Inc. J Appl Polym Sci 100: 3877–3888, 2006

Key words: blends; compatibilization; crosslinking; graft copolymers; NMR

INTRODUCTION

Polymer blends are an important class of materials, because they may exhibit synergistic effects with respect to useful properties. They may be generally categorized into two main classes: immiscible blends and miscible blends. Immiscible blends are those that exist in two different phases, for example, rubber-toughened plastics. On the other hand, miscible blends are those that exist in a single homogeneous phase and may exhibit different properties that are uncommon to either of the pure components. Apart from these two, there is a third category of blends, often called *technologically compatible blends* or *alloys.* The latter are those that exist in two or more different phases on a microscale but that exhibit macroscopic properties similar to that of a single-phase material.[1,2] Unfortunately, most polymer blends are thermodynamically immiscible, which results in poor interfacial adhesion and a gross, phase-separated morphology; this consequently leads to poor mechanical properties. It is already well known that the phase morphology of immiscible polymer blends can be influenced by the use of appropriate compatibilizers, block or graft copolymers, which can act as interfacial agents. The basic roles of the compatibilizers are the reduction of interfacial tension, the enhancement of interfacial adhesion, finer dispersion, and the improvement of morphological stability.

Block or graft copolymer compatibilizers can be premade and added to immiscible polymer blends but can also be generated in situ through covalent or ionic bonding (chemical reaction) during the reactive melt-blending process. The latter is a very effective means of compatibilization because the compatibilizers are formed at the site where they are required to be present: at the interface. In general, both polymers have to be functionalized with chemical groups that show reactivity toward each other.[3]

There is a possibility of the formation of comb-like in situ grafts of polypropylene (PP) with ethylene–propylene–diene terpolymer (EPDM) at the interface during the process of dynamic crosslinking in coagent-assisted, peroxide-cured PP/EPDM blends. These in situ graft links can act as a compatibilizer in such a system, which in turn, can improve the final mechan-

ical properties of the blends. Very recently, Isayev[4] reported the in situ compatibilization of plastic/rubber and rubber/rubber blends through ultrasonic treatment of the blends with continuous mixing. However, in our preliminary study, we found it very difficult to prove the in situ generation of graft links formed during dynamic crosslinking by conventional characterization techniques, such as Fourier transform infrared (FTIR) spectroscopy, differential scanning calorimetry, or dynamic mechanical thermal analysis (DMTA), because of the extremely low number of graft links formed.

Extensive studies on PP/EPDM thermoplastic elastomeric olefins (TEOs) have been carried out by several authors because a wide range of properties can be obtained just by changing the blend composition.[5–10] PP and EPDM are considered incompatible, although their molecular structures are very similar. A number of studies have been carried out on the impact modification of polyolefins by the addition of various elastomers,[11–13] for instance, EPDM or styrene–ethylenebutylene–styrene (S–EB–S).

However, only limited work has been published so far about the use of compatibilizers for PP/EPDM TEOs and thermoplastic vulcanizates (TPVs). The addition of 2–15 wt % of an ethylene–propylene block copolymer containing 80–90 wt % propylene has been tried recently as a compatibilizer to improve the dispersion of EPDM in PP for PP/EPDM TEOs.[14] Lohse et al.[15] reported that the addition of a small amount, less than 10 wt %, of isotactic polypropylene (iPP)–EPDM graft copolymer to an iPP/ethylene propylene copolymer (EPM) TEO had a pronounced effect on its morphology and final mechanical properties. The miscibility between PP and EPDM was also found to improve through the introduction of specific interactions, for instance, dipole ion interaction: PP was modified by the grafting of maleic anhydride onto the backbone, which led to maleic anhydride grafted PP; on the other hand, sulfonated EPDM ionomer neutralized with bivalent zinc cations was used as the other component. Ludwig and Moore[16] observed an increase in low-temperature impact strength and an enhanced dispersion of EPDM in the PP matrix in the presence of a peroxide initiator and a new multifunctional coupling agent, hexa(allylamino) cyclotriphosphonitrile. It has also been reported that the miscibility of PP/EPDM blends can be controlled by the addition of an ethylene-co-methacrylic acid ionomer followed by the application of dynamic vulcanization.[17] Coran and Patel[18] showed that the morphology of a nitrile rubber/PP blend could be controlled by the addition of block copolymers, with compatibilizing segments for both of the polymers. Enhanced solubility, partitioning, and homogenizing effects ha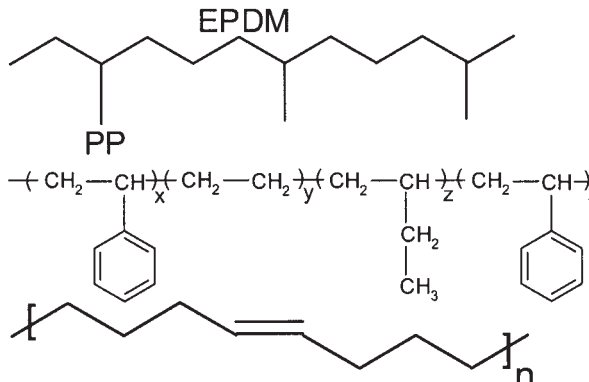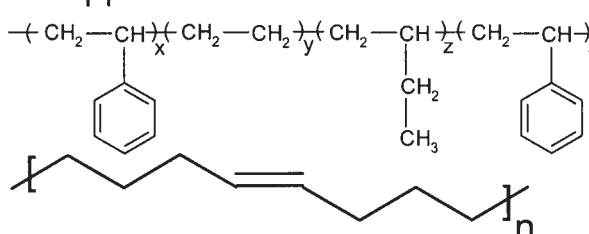ve also been achieved by the incorporation of commercial and model phenol and hydrocarbon resins in rubbers and corresponding blends.[19,20]

The basic objective of this study was to search for in situ compatibilization or graft links formed during the coagent-assisted peroxide vulcanization of PP/EPDM blends. For that purpose, the main focus was on NMR, as it was known that other more common techniques would not lead to conclusive results because of the very low number of graft links that were expected to be formed. An attempt was made to search for the existence of in situ formed graft link structures by the NMR cross-polarization/magic-angle spinning (CP-MAS) technique in terms of spectra and relaxation time [$T_{1\rho}$ (^{13}C)]. Various premade compatibilizers were also tested as references for PP/EPDM blends to obtain a quantified insight into the influences to be expected from in situ formed PP–EPDM graft links. Three potential compatibilizers for PP/EPDM blends were selected for that purpose: PP-grafted EPDM, S–EB–S, and trans-polyoctenamer (TOR). Apart from the PP–EPDM graft copolymer as described later, S–EB–S and TOR were tried as compatibilizers because they had solubility parameters that were close to that of PP and EPDM, respectively. S–EB–S acts as a compatibilizer in PP/PC,[21] polyethylene/polystyrene (PS),[22] polyethylene/polyamide (PA), PS/poly(ethylene terephthalate), and PS/PA blends and others,[23] improving the impact strength. On the other hand, Blume and Schuster[24] reported that 5 phr of TOR acts as a very good compatibilizer, improving the tensile strength and elongation at break, for peroxide-cured nitrile rubber/PP blends.

Solid-state NMR is now one of the most useful techniques for the characterization of polymers without the need to dissolve the polymers in suitable solvents. Important information about miscibility and compatibility, intermolecular interactions, molecular dynamics and morphology, crystal structures, and so on of polymer blends can be obtained by the examination of NMR parameters such as chemical shifts, line widths, relaxation parameters, and polarization transfer processes.[25–30] Until several decades ago, solid-state NMR provided spectra containing only broad lines. The introduction of the ^{13}C-NMR CP-MAS technique created lots of interest by providing insight into the structures of polymers, carbohydrates, biopolymers, and so on. Generally, magic-angle spinning refers to the combination of cross-polarization (CP), the actual rotation of the sample at the magic angle of 54.7°, and the dipolar decoupling of the ^{1}H nuclei from the ^{13}C nucleus. With rigid solid substances, only the combination of all three experiments makes it possible and practical to record spectra of rare nuclei (most commonly ^{13}C) and to resolve them in terms of chemical structure.[31]

$T_{1\rho}$ (^{13}C) in the rotating coordinate system is another special parameter for the investigation of polymers.

TABLE I
Chemical and Commercial Names and Structures of the Compatibilizers Used

Chemical and commercial names	Chemical structure
PP–EPDM graft copolymer	
S–EB–S, Kraton G (Kraton Polymers): Pure triblock copolymer with 35 wt % ethylene content and 20 wt % PS content TOR, Vestenamer 8012 (Degussa)	

The amplitude of the radio frequency field, which is applied during the relaxation and which is parallel to the magnetization, determines the frequency of the spins within the rotating coordinate system. Molecular motions or dynamics having a spectral component at this frequency are of vital importance for the relaxation. However, the interpretation of $T_{1\rho}(^{13}C)$ data is complicated because the relaxation in the rotating coordinate system is caused by the fluctuating dipole fields of the protons.

High-resolution ^{13}C-NMR spectra of solid iPP were studied extensively by Bunn et al.[32] They reported a dependence of the solid-state spectra on the history of the physical treatment of the sample and also a relationship of these spectra to the structure of the crystalline regions of the materials. iPP can exist in two different forms: the thermodynamically stable crystalline α form, consisting of iPP chains in a helical conformation packed in a monoclinic unit cell, and the metastable β form, containing hexagonally packed helical chains. Normally, the β form shows chemical shifts at a higher side compared to the α form. Investigations were carried out not only on the homopolymers but also, for instance, on PP grafted with butadiene to quantitatively determine the proportion of grafts via CP-MAS experiments.[33]

EXPERIMENTAL

Materials

Ethylidene norbornene containing EPDM rubber, which included 50 wt % paraffinic oil, was obtained from DSM Elastomers B.V. (Geleen, The Netherlands). The EPDM contained 63 wt % ethylene and 4.5 wt % ethylidene norbornene. It had a Mooney viscosity [ML (1+4)] at 125°C of 52. PP was obtained from DSM Polypropylenes B.V. (Geleen, The Netherlands). The

melt flow index of PP measured at 230°C and 2.16 kg was 0.3 g/10 min. Dicumyl peroxide (DCP; 40%) was used as the crosslinking agent and triallyl cyanurate (TAC; 50%) was used as the coagent and was obtained from Akzo Nobel Polymer Chemicals B.V. (Deventer, The Netherlands). Two stabilizers, Irganox 1076 and Irgafos 168, were obtained from Ciba Geigy Ltd. (Basel, Switzerland).

The chemical and commercial names and structures of the three different types of compatibilizers under investigation are given in Table I. PP–EPDM graft copolymer was synthesized in the laboratories of DSM Research B.V., whereas S–EB–S was a specially synthesized grade from Kraton Polymers (Louven-la-Neuve, Belgium).

Synthesis of PP–EPDM graft copolymer

A graft copolymer with iPP arms pendant from an ethylene–propylene copolymer backbone was synthesized according to the process as described by Lohse et al.[15] The synthesis involved a two-step process. In the first step, EPDM was prepared with vinylidene norbornene (VNB) as a diene so that there remained unreacted double bonds well removed from the polymer backbone. In the second step, iPP chains were allowed to grow from these double bonds to form the graft copolymer.

VNB-containing EPDM polymer was made first as follows: A continuous-flow stirred-tank reactor was used to synthesize VNB-containing EPDM. The temperature was kept at 35°C. A feed stream of hexane, ethylene, propylene, and VNB was continuously fed to the continuous-flow stirred-tank reactor. A Ziegler–Natta catalyst system consisting of vanadium oxitrichloride and ethylaluminum sesquichloride with an Al/V molar ratio of 5 was used to achieve a homoge-

neous polymer. The residence time in the reactor was 8 min. Hydrogen was added to act as a chain-transfer agent. The characteristics of the VNB-containing EPDM polymer were as follows:

- Ethylene content = 54.3 wt % and propylene content = 42.4 wt %, as calculated from a FTIR study calibrated with ^{13}C-NMR.[34]
- The FTIR spectra of the polymer film showed a band at 906 cm^{-1}, indicating the incorporation of VNB. VNB content = 3.2 wt %, as also obtained from the FTIR spectra calibrated with ^{1}H-NMR.[34]
- Molecular weights: number-average molecular weight (M_n) = 37,000 g/mol; weight-average molecular weight (M_w) = 105,000 g/mol; z-average molecular weight (M_z) = 280,000 g/mol. M_w/M_n = 2.9 and M_z/M_w = 2.7, which indicated a relatively narrow molecular weight distribution as measured by gel permeation chromatography.
- Mooney viscosity [ML (1+8)] at 100°C = 19.6.

The grafting of iPP on the EPDM polymer was achieved as follows:

1. The aforementioned VNB-containing EPDM was dissolved in 1000 mL of petroleum ether and then passed through a column of activated aluminum oxide to remove previously used vanadium catalyst. After evaporation of part of the solvent, 900 mL of petroleum ether solution of EPDM (2.1 g/100 mL) was obtained.
2. A 2-L flask was then charged by 750 mL of the EPDM-containing petroleum ether and 3 mL of triethyl aluminum (7M, 21 mmol) as a cocatalyst and then heated to a constant reaction temperature of 50°C. Titanium trichloride (2 g; Stauffer AA) was added as a catalyst. After that, gaseous propylene monomer was introduced to the flask at atmospheric pressure. After 0.5 h, the solution containing EPDM+iPP was then saturated by ethylene gas at atmospheric pressure. The latter was performed to initiate the grafting procedure: the catalyst used here could not effect a reaction between VNB and propylene but could only catalyze a reaction between VNB and ethylene for steric reasons, the smaller size of ethylene compared to propylene. The reaction mixture thus formed was stirred and allowed to react for 2 h. A suspension of white powder was obtained.
3. To the previously mentioned flask, 20 mL of HCl/methanol mixture and 200 mL of methanol were added. A methanol layer containing the catalyst residue was first removed. Methanol (300 mL) was then added to the petroleum ether layer, which already contained a white precipitate. Lots of precipitates were formed. After the

TABLE II
TEO Composition

Material	phr
EPDM[a]	200
PP	100
Compatibilizer	0–25

[a] Including 50 wt % paraffinic oil.

separation, two fractions were obtained: one was white precipitate, and the other one was the petroleum ether solution. The solvent was removed, and two polymers were finally obtained: PP–EPDM graft copolymer 1 (90 g) and PP–EPDM graft copolymer 2 (24 g). PP–EPDM graft copolymer 1 was selected as the compatibilizer. The specifications of the latter were as follows:

- Ethylene content = 5.7 wt % and propylene content = 94.3 wt % as calculated from FTIR analysis calibrated with ^{13}C-NMR.
- Molecular weights: M_n = 16,000 g/mol; M_w = 390,000 g/mol; M_z = 2,000,000 g/mol. M_w/M_n = 24.1 and M_z/M_w = 5.2, which indicated a broad molecular weight distribution as measured by gel permeation chromatography.
- FTIR film spectra of the graft showed a sharp band at 899 cm^{-1}, which indicated the presence of a high amount of iPP, and 721 cm^{-1}, which indicated the presence of EPDM. On the other hand, absence of a band around 906 cm^{-1} indicated the full reaction of VNB into the final grafted polymer.

Preparation of PP/EPDM TEOs and TPVs containing premade compatibilizers

The TEO and TPV compositions used are shown in Tables II and III. The experimental variable was the type and amount of the compatibilizers. All TPVs were mixed by a batch process in a Brabender Plasti-Corder PL-2000 (Duisburg, Germany) with a mixing chamber volume of 50 cm^3. The batch size was 36 g. The mixer temperature was kept at 180–200°C. A constant rotor (cam-type) speed of 80 rpm was applied. PP, stabilizers (Irganox 1076 and Irgafos 168), and EPDM rubber were first mechanically melt-mixed. After 4 min of mixing, the coagent (TAC) was added, followed by DCP. Mixing was continued for another 5 min to accomplish the dynamic vulcanization process. Immediately after mixing, the composition was removed from the mixer and, while still molten, passed once through a cold two-roll mill to achieve a sheet about 2 mm thick. The sheet was cut and pressed in a

TABLE III
TPV Composition

Material	phr
EPDM[a]	200
PP	100
Compatibilizer	0–25
DCP	10.1
TAC	5.0

[a] Including 50 wt % paraffinic oil.

compression-molding machine (Wickert, Germany) (WLP 1600/5 4/3 Wickert laboratory press at 200°C, 4 min and 125 bar of pressure). Aluminum foil was placed between the molded sheet and the press plates. The sheet was then cooled down to room temperature under pressure. The dimensions of the sheets were 90 × 90 × 2 mm. Test specimens were die cut from the compression-molded sheet and used for testing after 24 h of storage at room temperature. The TEOs were also prepared in the same way.

Testing procedures

Tensile tests

Tensile tests were carried out according to ISO 37 on dumbbell-shaped specimens (type 2) with a Zwick tensile testing machine (Z020) (Germany) at a constant crosshead speed of 500 mm/min. The Young's modulus was determined from the initial slope of the stress–strain curve (0.1–0.25% strain) at a crosshead speed of 50 mm/min. The hardness of the samples was measured by a Zwick hardness meter (Shore A type, ISO R868).

DMTA

DMTA measurements were performed on compression-molded samples (50 × 9 × 2 mm) with a Myrenne ATM3 torsion pendulum (Germany) at a frequency of 1 Hz and 0.1% strain. The samples were first cooled to −80°C and then subsequently heated at a rate of 1°C/min over a temperature range of −80 to 60°C. The tan δ peak maxima were assigned to the glass transitions of the EPDM and the PP.

Morphological characterization

The phase morphology of various PP/EPDM TEOs with the compatibilizers was investigated by low-volt-

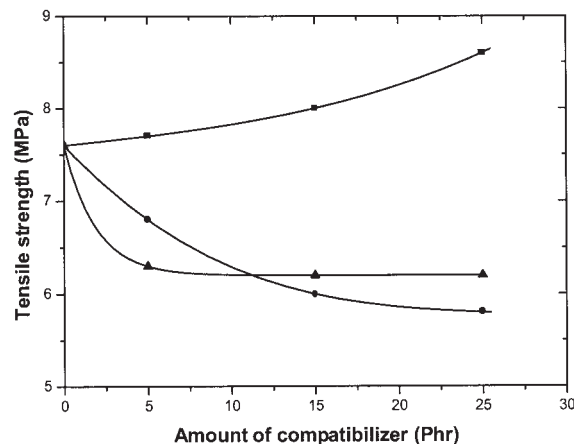**Figure 1** Measurement of $T_{1\rho}$ by CP via spin locking.

Figure 2 Tensile strength of PP/EPDM TEOs as a function of the amount of various compatibilizers: (■) PP–EPDM graft copolymer, (●) S–EB–S, and (▲) TOR.

age scanning electron microscopy (LV-SEM). For this study, a blend composition of 67 : 33 w/w of PP and EPDM was chosen (different from Table II) on purpose to achieve a well-dispersed phase morphology. The samples were quickly quenched in liquid nitrogen after they were taken out of the hot mixer. Afterward, they were cut cryogenically (at −130°C) to very thin slices (~50–80 nm) with a diamond knife in a Leica Ultramicrotome EM FCS (Wetzlar, Germany). The microtomed samples were vapor-stained with freshly prepared ruthenium tetroxide for 30 min to generate contrast between the PP and EPDM phases. The stained surfaces were then examined under LV-SEM. The images were obtained with a LEO 1550 FEG scanning electron microscope (UK) at an operating voltage of 0.65 kV.

Search for in situ graft links

Preparation of the samples

Thin films of PP, EPDM rubber, and DCP-cured PP/EPDM TPVs (made by the same recipe mentioned in Table III, only without the compatibilizer) were first prepared in a compression-molding machine, the WLP 1600/5 4/3 Wickert laboratory press at 200°C for 2 min and under 125 bar of pressure. Aluminum foil was placed between the molded film in the press plates. The films were then cooled down to room temperature under pressure. Later, the PP phase was extracted from the PP/EPDM TPV film by exhaustive hot xylene treatment in a Soxhlet apparatus. The extraction was assumed to be complete. In situ formed graft links together with degraded PP–oligomer branches were supposed to remain in the film even after the extraction. Only a limited number of experiments could be performed because of the restricted availability of the NMR technique.
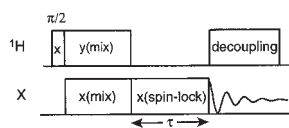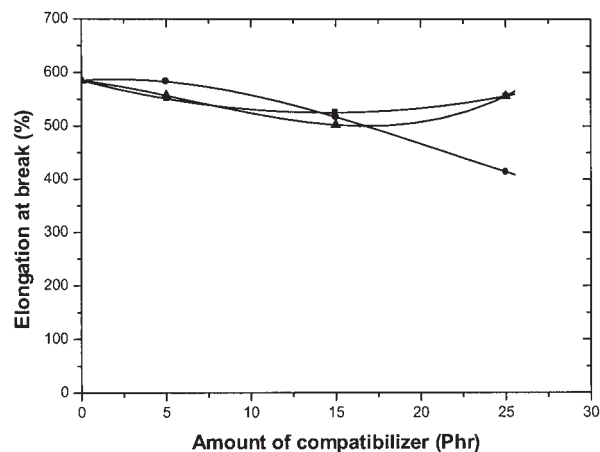
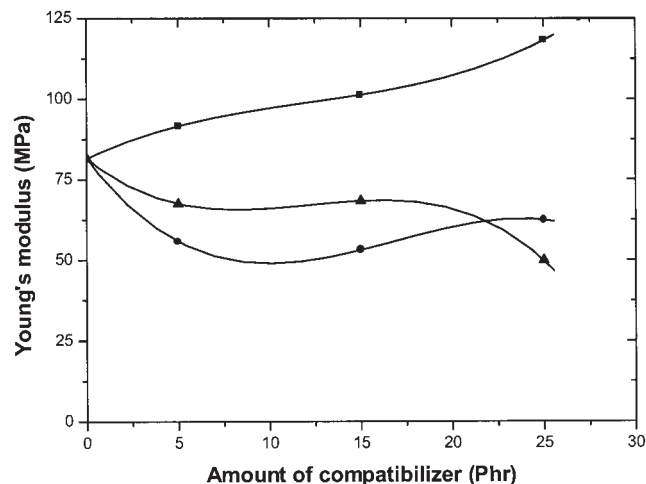**Figure 3** Elongation at break of PP/EPDM TEOs as a function of the amount of various compatibilizers: (■) PP–EPDM graft copolymer, (●) S–EB–S, and (▲) TOR.

Figure 5 LV-SEM micrograph of PP/EPDM (67:33 w/w) TEOs at higher magnification (scale: 300 nm).

Solid-state NMR

First, solid-state ^{13}C-NMR spectra of the thin films were obtained at 70°C with a Chemagnetics CMX-400 Infinity spectrometer (homebuilt, University of Nijmegen, The Netherlands) equipped with a CMX 4-mm BB CP-MAS rotor. NMR spectra were recorded with CP-MAS pulse sequence. In this sequence, the sample was rotated at very high speed (ca. 9 kHz) to average out the dipolar coupling and the chemical shift anisotopy. To gain sensitivity, proton magnetization was transferred to the carbons by means of CP. During the sampling of the signal, the protons were decoupled.

Second, the $T_{1\rho}$ (^{13}C) values in the rotating coordinate system were also measured at 70°C via the CP-MAS technique. The most intense signals as obtained from the first experiments were used to perform this

relaxation experiment. The magnetization was spin-locked in the xy plane, and the relaxation in this plane was measured, which was carried out by an increasing spin-lock time and subsequent measurement of the signal intensity, as shown in Figure 1.

The NMR signal intensity (M) was measured as a function of the spin-lock duration (τ). The time constants ($T_{1\rho}$'s), which are characteristic of different rates of the magnetization decay, were obtained by a least square fit of the data with a Weibull function or a linear combination of the Weibull function and exponential functions. Depending on the nature of system studied, one, two, or three components were used for the fit. Statistically, it was insignificant to use a series containing more than a three-component fit for this purpose. In the case of two different $T_{1\rho}$'s (short and long), the following equation was used:

Figure 4 Young's modulus of PP/EPDM TEOs as a function of the amount of various compatibilizers: (■) PP–EPDM graft copolymer, (●) S–EB–S, and (▲) TOR.
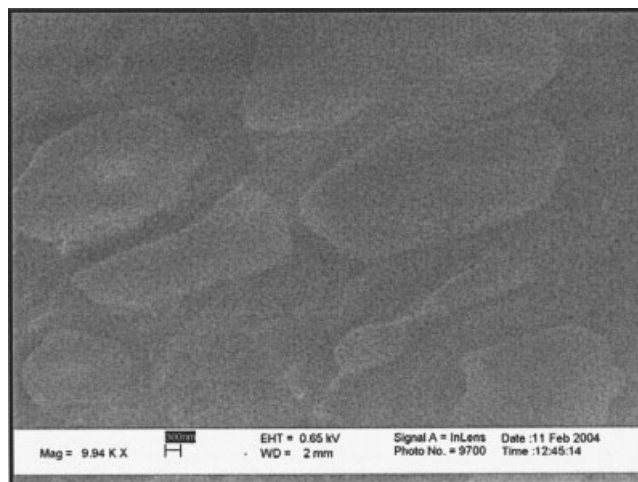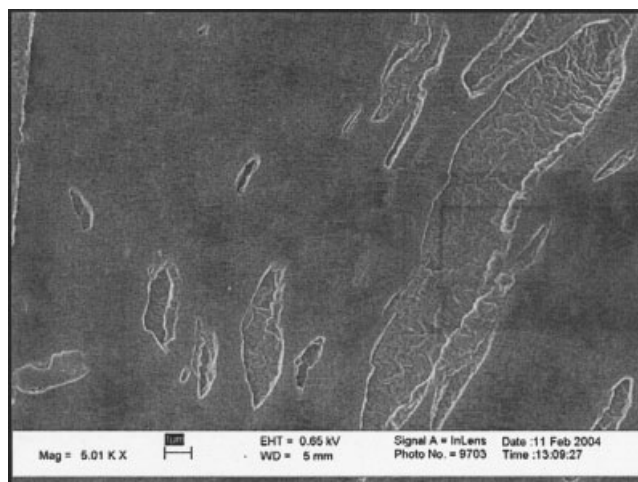

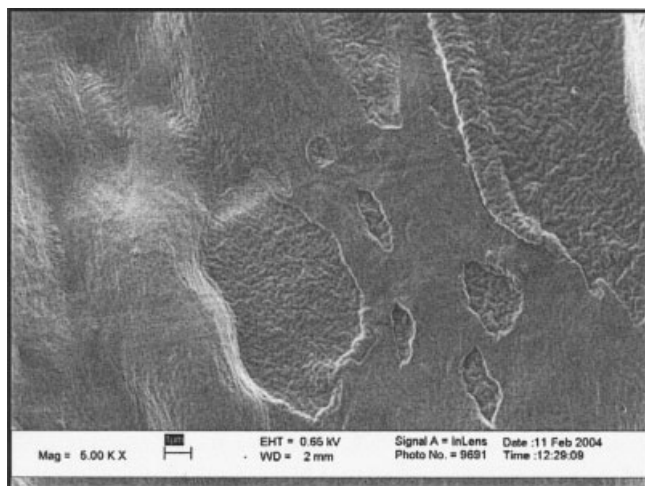**Figure 6** LV-SEM micrograph of PP/EPDM (67:33 w/w) TEOs at lower magnification (scale: 1 μm).

Figure 7 LV-SEM micrograph of PP/EPDM TEOs in the presence of PP–EPDM graft copolymer (scale: 1 μm).

$$M = M_\infty + (M_0 - M_\infty)e^{\frac{-\tau}{T_{1\rho}^l}} + (M_0 - M_\infty)e^{\frac{-\tau}{T_{1\rho}^l}} \quad (1)$$

where M_0 is the initial magnetization and M_∞ is the magnetization when the spin system and the lattice reach a quasiequilibrium during the spin lock ($M_\infty = 0$ at resonance). $T_{1\rho}$ measurement is suitable to measure correlation times on the order of kilohertz, in our case about 80 KHz, because this value is particularly useful for probing molecular motions of polymers.

RESULTS AND DISCUSSION

Influence of various premade compatibilizers on the physical properties of the TEOs

Figure 2 shows the tensile strength of TEOs with various premade compatibilizers as a function of their

amounts. With increasing PP–EPDM graft copolymer, the tensile strength increased. On the other hand, for S–EB–S, the tensile strength decreased, whereas for TOR, it first decreased and then reached a plateau.

Figure 3 shows the elongation at break as a function of concentration of the compatibilizers. With increasing concentration, the elongation at break decreased somewhat in all cases. Overall, small differences between the various compatibilizers were observed, except for S–EB–S, which showed a relatively low elongation at break compared to the others at a concentration of 25 phr of the compatibilizer.

In Figure 4, the Young's modulus as a function of amount of the compatibilizers is shown. The Young's modulus increased with increasing concentration of the PP–EPDM graft copolymer. On the contrary, for S–EB–S and TOR a decrease was observed.

All these results clearly indicate that the PP–EPDM graft copolymer acted as an effective compatibilizer in PP/EPDM TEOs because its addition improved the physical properties, such as tensile strength and modulus, to a considerable extent. In contrast, S–EB–S and TOR did not contribute to the improvement of the physical properties and thereby did not act as good compatibilizers in the PP/EPDM blends. An obvious explanation for the better performance of the PP–EPDM graft copolymer was the fact that it most closely structurally resembled that of the two constituents of the blend: PP and EPDM.

Influence of various premade compatibilizers on the morphology of the TEOs

Figures 5 and 6 show the LV-SEM micrographs of PP/EPDM (67 : 33 w/w) TEOs without the addition of
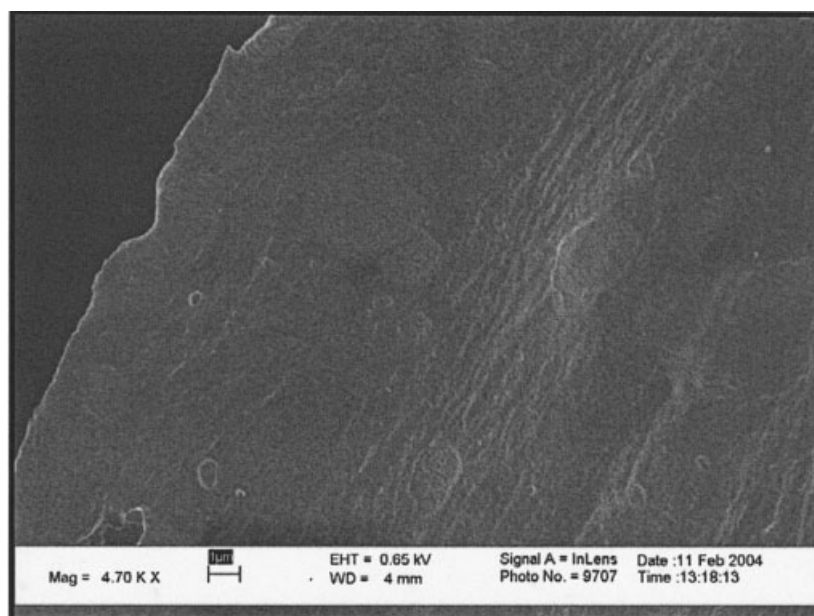

Figure 8 LV-SEM micrograph of PP/EPDM TEOs in the presence of S–EB–S (scale: 1 μm).
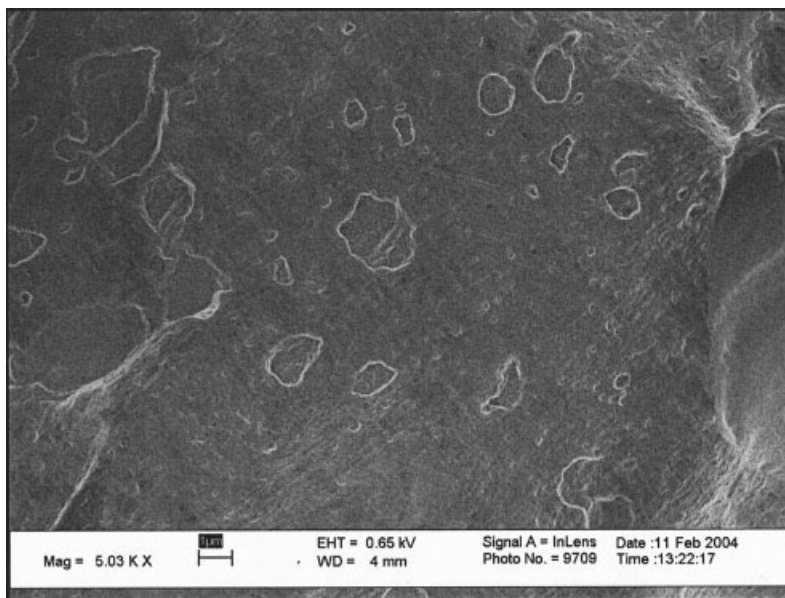
Figure 9   LV-SEM micrograph of PP/EPDM TEOs in the presence of TOR (scale: 1 μm).

any compatibilizer: EPDM particles dispersed and distributed in the continuous PP matrix. The structured EPDM particle sizes mostly varied between 3 and 5 μm. LV-SEM images of PP/EPDM TEOs after the addition of the compatibilizers PP–EPDM graft copolymer, S–EB–S, and TOR are depicted in Figures 7–9, respectively. A slight reduction of EPDM particle size up to mostly about 1.5–2 μm was noticed in all of the cases, which indicated some action of compatibilization.

Influence of the PP–EPDM graft copolymer as a compatibilizer on the dynamic mechanical properties of the TEOs

Figure 10 shows the DMTA results of PP/EPDM TEOs with and without the addition of the PP–EPDM graft copolymer. As shown in the plot of the loss angle tan δ as a function of temperature, there were two major transitions: the glass-transition temperature (T_g) of EPDM around $-56°C$ and that of PP around $-10°C$. After the addition of the PP–EPDM graft copolymer to the PP/EPDM TEO, a slight decrease in the peak height of tan δ was observed for EPDM, a slight shifting of the T_g of PP toward lower temperature and a broadening of the T_g peak. These observations were an indication of a slight improvement in the compatibility between PP and EPDM under the influence of the PP–EPDM graft copolymer in line with the mechanical properties.

Influence of various premade compatibilizers on the physical properties of the TPVs

Figure 11 shows the tensile strength versus the concentration of the premade compatibilizers. In all cases,

tensile strength decreased with increasing amount of compatibilizers. In most cases, the values of the tensile strength of the PP/EPDM TPVs were even lower than those of the corresponding TEOs, regardless of the nature of compatibilizer. S–EB–S exhibited the lowest values, whereas TOR still showed the highest. The values obtained for the PP–EPDM graft copolymer varied between TOR and S–EB–S.

Figure 12 depicts the elongation at break as a function of the amount of the various compatibilizers. Hardly any difference in the values between TOR and S–EB–S was noticed for all concentrations of the compatibilizers. The elongation at break decreased with increasing amount of the PP–EPDM graft copolymer, which also showed the lowest values among all.

Young's modulus as a function of the amount of the compatibilizer is shown in Figure 13. In the case of
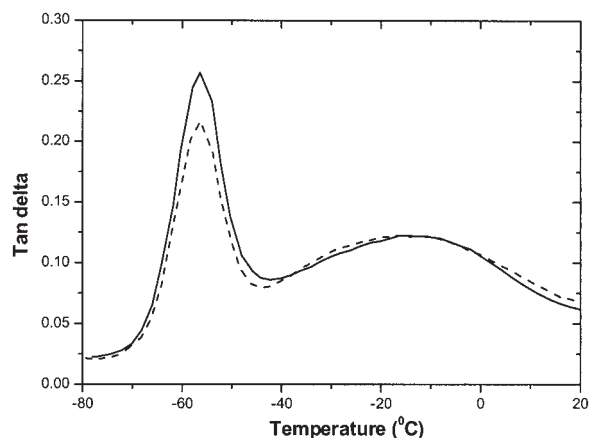

Figure 10   Tan δ as a function of the temperature of PP/EPDM TEO (—) without and (- - -) with the addition of 25 phr of PP–EPDM graft copolymer.
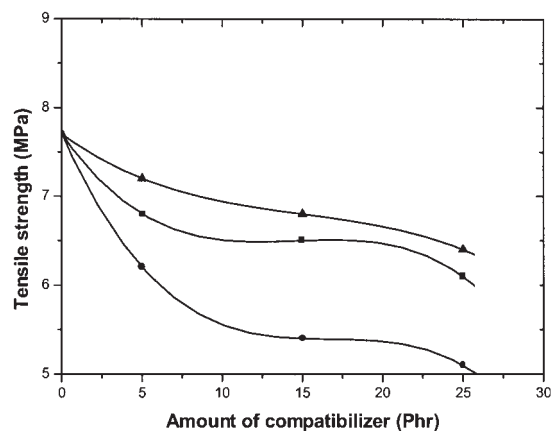
Figure 11 Tensile strength of PP/EPDM TPVs as a function of the amount of various compatibilizers: : (■) PP–EPDM graft copolymer, (●) S–EB–S, and (▲) TOR.

Figure 13 Young's modulus of PP/EPDM TPVs as a function of the amount of various compatibilizers: (■) PP–EPDM graft copolymer, (●) S–EB–S, and (▲) TOR.

S–EB–S and TOR, the Young's modulus decreased with increasing concentration of the compatibilizers. In contrast, for the PP–EPDM graft copolymer, the modulus kept increasing with the amount.

The aforementioned results reveal that although PP–EPDM graft copolymer acted as a good compatibilizer for the TEOs, it did not play the same role in the PP/EPDM TPVs. The most plausible reason was that DCP also reacted with the PP phase present in the graft copolymer itself, causing degradation, which finally led to the deterioration of physical properties such as tensile strength. However, the addition of the PP–EPDM graft copolymer improved the Young's modulus of the TPVs to some extent because of the incorporation of more overall PP in the blend, which came from the graft copolymer itself. S–EB–S failed again to act as an effective compatibilizer in the case of the TPVs, like in the TEOs. The slight improvement in
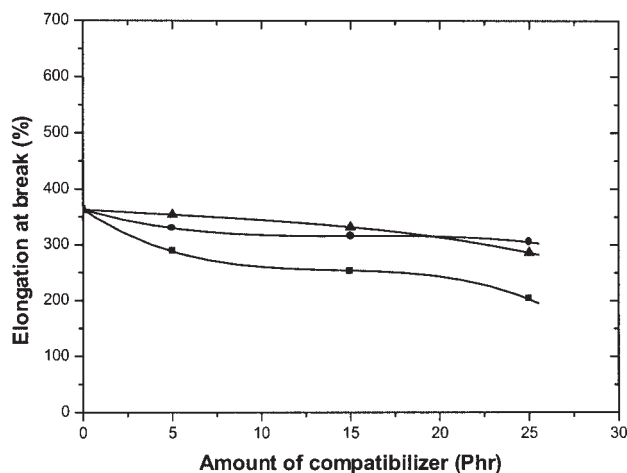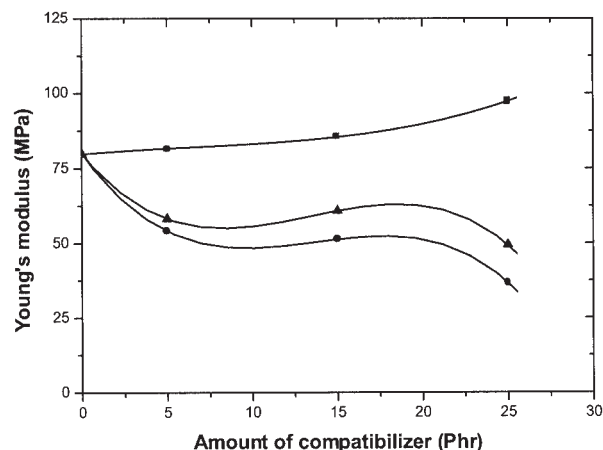
the physical properties, for example, tensile strength and Young's modulus, of TOR-containing TPVs compared to the corresponding TEOs, was most probably due to the dynamic crosslinking of the TOR itself through DCP.

These results clearly show that experiences gained with compatibilizers in unvulcanized TEOs could not simply be translated to TPVs. The vulcanization step, particularly the possible side reactions when peroxides were used, may have caused a complete reversal of effects. Because of the poor results obtained with these premade compatibilizers in TPVs, this approach was not further pursued with morphological and rheological characterizations.

Evidence for in situ compatibilization with the TPVs

Solid-state ^{13}C-NMR spectra

Solid-state ^{13}C-NMR spectra of PP, EPDM rubber, and a PP-extracted TPV sample, which may have contained the in situ formed PP–EPDM grafts, are shown
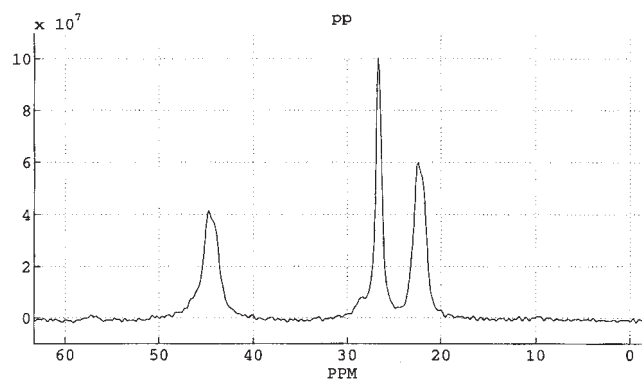

Figure 12 Elongation at break of PP/EPDM TPVs as a function of the amount of various compatibilizers: (■) PP–EPDM graft copolymer, (●) S–EB–S, and (▲) TOR.

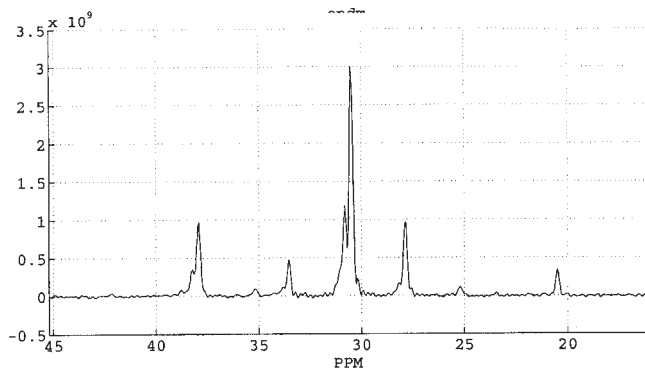**Figure 14** Solid-state ^{13}C-NMR spectrum of PP at 70°C.

Figure 15 Solid-state ^{13}C-NMR spectrum of EPDM at 70°C.

in Figures 14–16, respectively. Table IV shows the observed ^{13}C chemical shifts of the main peaks and the corresponding assignments for PP. The chemical shifts and corresponding assignments of various groups for EPDM rubber containing 50 wt % paraffinic oil are shown in Table V.

The ^{13}C spectra of the sample, PP extracted TPV, showed almost all of the main peaks, as shown in Table V, for EPDM rubber. In addition, it exhibited two other chemical shifts at 22.0 and 26.5 ppm, which indicated the presence of —CH$_3$ and —CH— from iPP. Thus, there was an indication that during the dynamic vulcanization process, PP–EPDM graft links were generated that still remained in the system even after the extraction of the PP phase from the TPV, with the assumption that the extraction was complete.

$T_{1\rho}$ (^{13}C) in the rotating coordinate system

The signal intensity obtained from the highest intensity peak of the spectra as a function of spin-lock duration for calculating the $T_{1\rho}$ values from the curve fitting for PP, EPDM rubber, and PP extracted TPV are depicted in Figures 17–19, respectively. The figures for other peaks of the spectra are not very clear because of
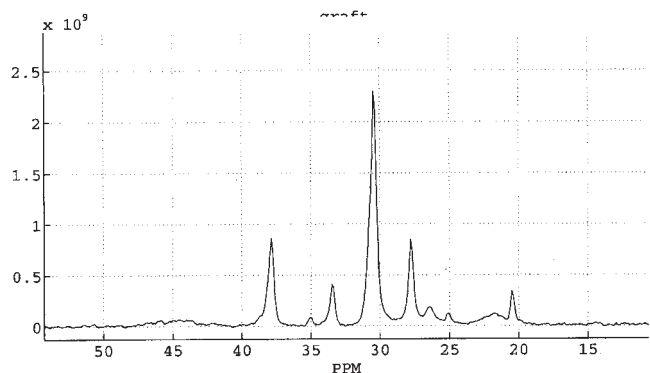

Figure 16 Solid-state ^{13}C-NMR spectrum of PP-extracted TPV at 70°C.

TABLE IV
Main Peaks of PP

Chemical shift (ppm)	Carbon type
43.8	—CH$_2$—
25.9	—CH—
21.6	—CH$_3$

their poor signal-to-noise ratio. All of the figures show that after the excitation of all transitions, the relaxation processes in the rotating frame could basically be fitted with an equation that was biexponential in nature. Table VI shows the short and long $T_{1\rho}$'s of different polymers. Consequently, PP showed two different rates of decay, which gave rise to two different $T_{1\rho}$ values. This could be taken as an indication that the PP contained two different domains: amorphous and crystalline. The amorphous phase, with a high mobility, showed a long $T_{1\rho}$ indicative of a slower relaxation process. On the other hand, the crystalline phase, with more rigidity, relaxed at a faster rate, which led to a relatively shorter $T_{1\rho}$. EPDM rubber could also be fitted with a biexponential decay function, which indicated the presence of highly mobile paraffinic oil showing a long $T_{1\rho}$ value. EPDM was mostly amorphous in nature and, thereby, showed a long $T_{1\rho}$, and the $T_{1\rho}$'s were longer as compared to that of PP. PP-extracted TPV, which did not contain oil anymore because xylene also extracted the oil, showed a different trend compared to normal EPDM because it showed two different types of relaxations. This indicated that probably due to the formation of crosslinks in the EPDM phase and in situ PP–EPDM graft links along with degraded PP–oligomer branches, which imparted more rigidity to the system, the relaxation occurred at a somewhat faster rate than EPDM.

CONCLUSIONS

During the dynamic vulcanization of PP/EPDM blends with DCP/TAC, there was the possibility of the generation of in situ graft links at the interface between both phases. Three potential compatibilizers (PP-grafted EPDM, S–EB–S, and TOR) for PP/EPDM blends were first investigated as references to obtain a quantified insight into the effects to be expected from

TABLE V
Main Peaks of EPDM Plus Oil

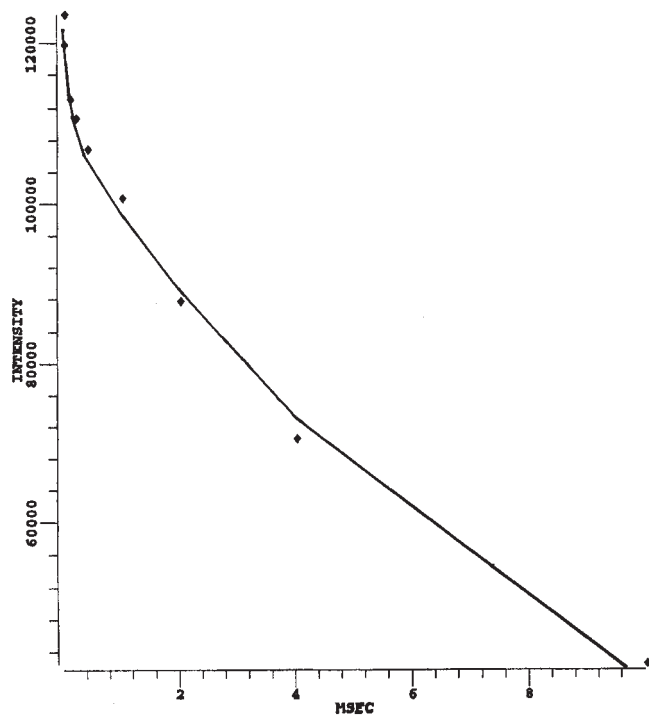| Chemical shift (ppm)	Carbon type
20.5	—CH$_3$
27.9	—CH$_2$—
31.0	—CH$_2$—
33.5	—CH$_2$— or —CH—
38.0	—CH$_2$—

Figure 17 Relaxation decay of the magnetization of PP at 70°C with the peak at 25.9 ppm.
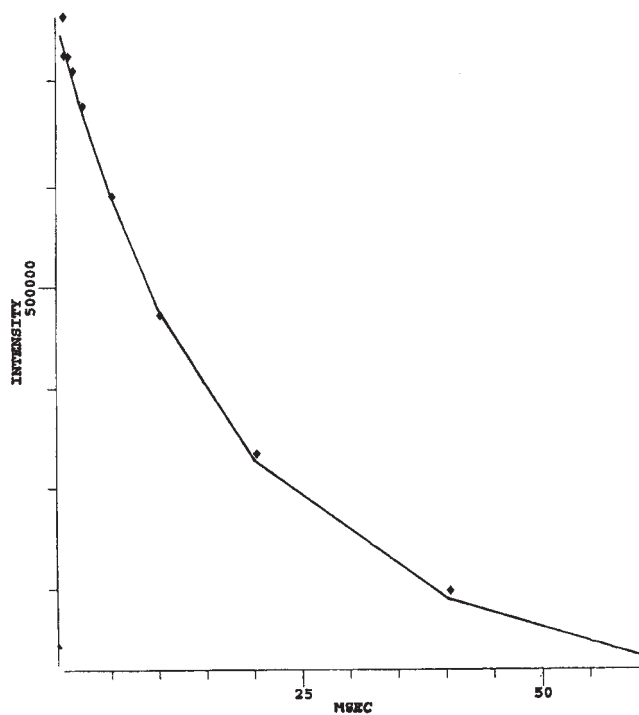

Figure 19 Relaxation decay of the magnetization of PP-extracted TPV at 70°C with the peak at 30.4 ppm.

in situ graft links. Only the first one showed some compatibilizing action in straight, unvulcanized blends, as evidenced by a slight increase in the tensile strength of the blend and a somewhat smaller EPDM particle size within the PP matrix. Also, dynamic mechanical testing, in particular T_g's of the PP and EPDM

components, showed some signs of compatibilization. The PP-grafted EPDM resembled most closely the structures of PP and EPDM. On the other hand, when mixed into a dynamically vulcanized PP/EPDM blend, all of the compatibilizers resulted in an overall deterioration in the mechanical properties. The vulcanization step, particularly with peroxides, caused a complete reversal of the effects observed with straight blends.

From the spectra obtained with high-temperature, solid-state NMR, there was an indication that PP–EPDM graft links were generated during the dynamic vulcanization process that still remained after the extraction of the free PP phase from the TPV film. However, the restriction must be made that some PP for another possible reason may have remained in the TPV after the extraction was considered complete. NMR relaxation experiments gave further evidence for the in situ formed graft links. In all cases, only qualitative indications could be achieved because of the extremely low number of graft links formed.
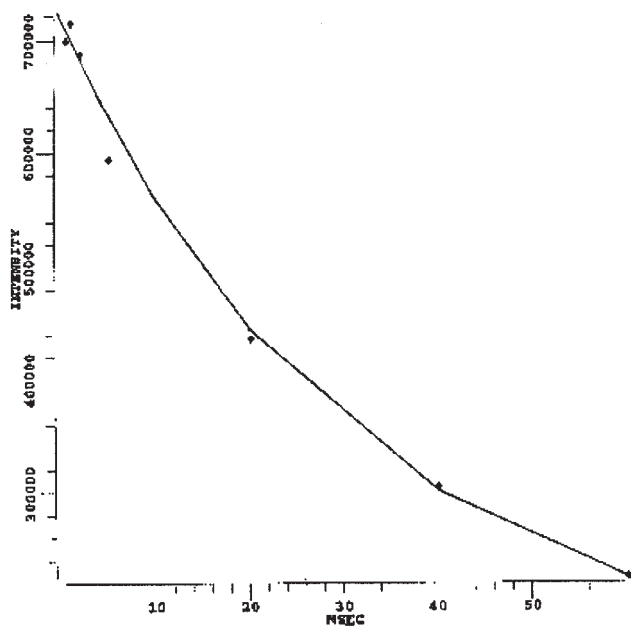

Figure 18 Relaxation decay of the magnetization of EPDM at 70°C with the peak at 30.5 ppm.

TABLE VI
Short and Long $T_{1\rho}$'s: of the Different Polymers

Polymer	Short $T_{1\rho}$ (ms)	Long $T_{1\rho}$ (ms)
PP	0.0001	0.0100
EPDM	0.0296	0.3971
PP-extracted TPV	0.0153	0.0906

References

1. Paul, D. R.; Newman, S. Polymer Blends; Academic: New York, 1978; Vols. I and II.
2. Utracki, L. A. Polymer Alloys Blends: Thermodynamics and Rheology; Hanser: Munich, 1990.
3. Datta, S.; Lohse, D. J. Polymeric Compatibilizers: Uses and Benefits in Polymer Blends; Hanser: Munich, 1996.
4. Isayev, A. I. Presented at the American Chemical Society Rubber Division Meeting, October 2002, Pittsburgh, PA.
5. Ho, W. J.; Salovey, R. Polym Eng Sci 1981, 21, 839.
6. Danesi, S.; Porter, R. S. Polymer 1978, 19, 448.
7. Dorazio, L. D.; Greco, R.; Martuscelli, E.; Rogosta, G. Polym Eng Sci 1983, 23, 489.
8. Karger-Koscis, J.; Kallo, A.; Szafner, A.; Bordor, G.; Senyi, Z. Polymer 1979, 20, 37.
9. Kalfoglou, N. K. J Macromol Sci Phys 1983, 22, 343.
10. Karger-Koscis, J.; Kallo, A.; Kuleznev, N. Polymer 1984, 25, 279.
11. Galli, P.; Dansei, S.; Simonazzi, T. Polym Eng Sci 1984, 24, 544.
12. Ha, C. S.; Kim, S. C. J Appl Polym Sci 1989, 37, 317.
13. Thermoplastic Elastomer: A Comprehensive Review; Legge, N. R.; Holden, G.; Schroeder, H. E., Eds.; Hanser: Munich, 1987.
14. Kaufman, G. L.; Dharmarajan, R. N.; Cozewith, C.; Ellul, D. M. (to Advanced Elastomer Systems). U.S. Pat. 9,094,995 (1998).
15. Lohse, D. L.; Datta, S.; Kresge, E. N. Macromolecules 1991, 24, 561.
16. Ludwig, K. N.; Moore, R. B. J Elast Plast 2002, 34, 171.
17. Kim, Y.; Cho, W. J.; Ha, C. S. Polym Eng Sci 1995, 35, 1592.
18. Coran, A. Y.; Patel, R. P. Rubber Chem Technol 1983, 56, 1045.
19. Schuster, R. H.; Schmidt, R.; Pampus, G.; Abendroth, H.; Umland, H. Kautsch Gummi Kunstst 1989, 42, 582.
20. Schuster, R. H.; Thielen, G.; Hallensleben, M. L. Kautsch Gummi Kunstst 1991, 44, 232.
21. Srinivasan, K. R.; Gupta, A. K. J Appl Polym Sci 1994, 53, 1.
22. Fayt, R.; Jerome, R.; Teyssie, P. J Polym Sci Part B: Polym Phys 1989, 27, 775.
23. Modic, M. J.; Pottick, L. A. Polym Eng Sci 1993, 33, 819.
24. Blume, M.; Schuster, R. H. Kautsch Gummi Kunstst 2003, 56, 114.
25. Cheung, T. T. T. Phys Rev B 1981, 23, 1404.
26. Schmidt-Rohr, K.; Clauss, J.; Blumich, B.; Spiess, H. W. Magn Reson Chem 1990, 28, s3.
27. White, J. L.; Mirau, P. Macromolecules 1993, 26, 3049.
28. Cho, G. Can J Chem 1994, 72, 2255.
29. Kimura, T.; Neki, K.; Tamura, N.; Horii, F.; Nakagawa, M.; Odani, H. Polymer 1992, 33, 493.
30. Kulik, A. S.; Haverkamp, J. Polymer 1995, 36, 427.
31. Voelkel, R. Angew Chem Int Ed Engl 1988, 27, 1468.
32. Bunn, A.; Cudby, M. E. A.; Harris, R. K.; Packer, K. J.; Say, B. J. Polymer 1982, 23, 694.
33. Barron, P. F.; Busfield, W. K.; Buchanan, T. M. Polymer 1983, 24, 1252.
34. Noordermeer, J. W. M. Kautsch Gummi Kunstst 1996, 49, 521.